

Radiation Dose Calculation Analysis During The Dismantling of Disused Sealed Radioactive Sources at CNESTEN: MCNP Code Simulation Results

B. El Azzaoui^{1,2*}, O. Kabach¹, R. Outayad², M. Y. Messous², K. Bergaoui³, K. Nbaoui¹, J. Kadiri¹, E. Chakir¹, E. Alibrahmi¹, A. Kharchaf¹

¹Materials Physics and Subatomics Laboratory, Physics Department, University Ibn Tofail, Kenitra, Morocco

²National Center for Energy, Sciences and Nuclear Techniques (CNESTEN), Rabat, Morocco

³National Center of Nuclear Sciences and Technologies, Technopole Sidi Thabet, Tunisia

ARTICLE INFO

Article history:

Received 4 May 2024

Received in revised form 8 June 2024

Accepted 1 July 2024

Keywords:

DSRSs
Dismantling
Radiological safety
MCNP
⁶⁰Co

ABSTRACT

Disused Sealed Radioactive Sources (DSRS) present significant risks of radiation exposure and environmental contamination during dismantling. Despite their sealed nature, DSRS can emit ionizing radiation, necessitating careful management to mitigate health risks. This article presents the MCNP simulation results of dosimetric operational quantities, namely Hp(3), Hp(10), and H(0.07), for hands and feet. This study focuses on a ⁶⁰Co source, due to its high radiation energy levels and widespread use in various socioeconomic sectors. The assessment of radiation exposure levels enabled the improvement of occupational radiation protection measures related to critical areas and steps in the dismantling process. According to the obtained results with the ⁶⁰Co source at its initial activity, and considering the maximum task duration, the dismantling process contributes to approximately 72.35 % of the daily dose limit of 80 μSv for worker category A, for the whole body. Therefore, these findings can contribute to a better understanding of radiation exposure risks and confirm compliance with regulatory requirements.

© 2024 Atom Indonesia. All rights reserved

INTRODUCTION

Disused Sealed Radioactive Sources (DSRS) refer to radioactive materials that are no longer used or required for their original purpose. They are enclosed within sealed containers to prevent radiation leakage [1,2]. These sources are commonly utilized in various fields such as medicine, industry, research, and agriculture for applications like cancer treatment, sterilization, and quality control. DSRS encompasses a diverse array of radioactive isotopes and materials used in devices such as radiography machines, industrial gauges, and laboratory equipment [3-6].

The hazards and challenges associated with DSRSs arise from the potential risks of radiation exposure and environmental contamination [7]. Despite being sealed, DSRS can emit ionizing

radiation, which poses significant health risks if not properly managed. Mishandling of shielding can result in high levels of exposure, while loss of control can lead to orphan sources, causing accidental exposure and environmental contamination. Exposure to radiation from DSRSs can cause acute effects such as radiation burns and radiation sickness, as well as long-term health consequences like an increased risk of cancer and genetic mutations. Challenges in managing DSRSs include ensuring secure storage, preventing unauthorized access, and addressing the risks of leakage or damage to the sealed containers over time [6,8,9]. Dismantling and effectively managing DSRSs is vital for minimizing the risks associated with these materials and ensuring public safety and environmental protection. Dismantling DSRS principal involves safely removing the radioactive material from its sealed container, as explained in Fig. 1, which reduces the potential for radiation exposure and environmental contamination.

*Corresponding author.

E-mail address: brahim.elazzaoui1@uit.ac.ma

DOI: <https://doi.org/10.55981/aij.2024.1469>

Proper management practices, including inventory tracking, secure storage, and regulatory oversight, are essential to prevent the loss, theft, or mishandling of DSRs [10,11]. By prioritizing dismantling and implementing robust management strategies, stakeholders can mitigate the hazards posed by DSRs and uphold the principles of radiation safety and security [12].



Fig. 1. DSRs dismantling operation principle.



Fig. 2. DSRs Dismantling workplace at CNESTEN [6].

In the context of dismantling, the radiological exposure is considered a planned exposure. After each campaign, a safety assessment has to be made, to optimize the exposure and ensure the compliance with regulatory framework. In this study, the objective is to evaluate the radiological exposure associated with the dismantling of DSRs and ensure that workers' exposure meets the requirements outlined in regulatory documents and international standards for radiation safety [13,14]. Additionally, we aim to explore an effective occupational radiation protection plan to minimize worker exposure in the dismantling process (see Fig. 2). While the dismantling of alpha and beta emitters may not require specific protocols, handling gamma emitters with high energy and activity levels necessitates stringent measures. Therefore, we conducted an investigation using ^{60}Co , due to its wide utilization in various socioeconomic sectors, considering its energy level and emissions [15].

As the only organization responsible for collecting and managing radioactive waste, the National Center for Energy, Sciences, and Nuclear Techniques (CNESTEN) in Morocco has adopted

the dismantling process for the treatment of DSRs. CNESTEN has an extensive experience in this area through collaboration with the International Atomic Energy Agency (IAEA). Additionally, CNESTEN is dedicated to advancing nuclear research and development. Its mission includes promoting the peaceful use of nuclear technology, operating the TRIGA Mark II research reactor, and ensuring safety standards.

The evaluation of the radiological risks is based on the simulation of operational quantities, which are defined as "equivalent doses." These quantities are considered upper estimators of protection quantities namely equivalent dose and effective dose (HT, E) for highly and weakly penetrating radiations [16-19]. They are measurable by instruments equipped with radiation detectors. These quantities, Hp(3), Hp(10), and H(0.07) at hands and feet, are calculated by MCNP code in various exposed tasks during the dismantling process using conversion coefficients from fluence to equivalent dose [20,21].

MATERIAL AND METHOD

MCNP code

The MCNP code, developed at the Los Alamos National Laboratory, serves as a versatile tool designed to track a wide spectrum of particles, including neutrons, electrons, photons, and more, across a broad energy range [22]. In our research, we utilized MCNP to simulate various exposed situations including the radioactive source, work conditions, and detectors in potentially exposed areas in the personal body. Personal operational quantities are simulated using the F5 tally, which gives an output as flux at a point or ring detector, measured in units of particles per square centimeter (N/cm^2). By applying the multiplication function Fm, this card allows the conversion of tally results into different quantities, such as dose or energy deposition, for example, to normalize the source activity and facilitate the time conversion unit. To obtain the equivalent dose rate in sieverts per hour (Sv/h), the DF (Dose Function) card was used in conjunction with the DE (Dose Energy) card to apply the ICRU conversion coefficients to the tally results.

Simulated material

In this study, the walls of the dismantling laboratory were simulated using ordinary concrete.

The shielding for the radioactive source was simulated using lead, the table was simulated using stainless steel, and the operator's shielding protection was simulated using lead and lead glass. The characteristics of the materials used are defined in Table 1.

Table 1. The characteristics of used materials [23].

Elements	Ordinary concrete	Lead	Lead glass	Stainless steel 304
H	0.022100	-	-	-
C	0.002484	-	-	0.000400
O	0.574930	-	0.156453	-
Na	0.015208	-	-	-
Mg	0.001266	-	-	-
Al	0.019953	-	-	-
Si	0.304627	-	0.080866	0.005000
K	0.010045	-	-	-
Ca	0.042951	-	-	-
Fe	0.006435	-	-	0.701730
Ti	-	-	0.008092	-
As	-	-	0.002651	-
Pb	-	1	0.751938	-
P	-	-	-	0.000230
S	-	-	-	0.000150
Cr	-	-	-	0.190000
Mn	-	-	-	0.010000
Ni	-	-	-	0.092500
Density (g/cm ³)	2.300000	11.3500	6.220000	8.00000

Investigated source: ⁶⁰Co

The source utilized in this study is an isotropic source of ⁶⁰Co, manufactured on July 14, 1992, with an initial activity of 3.7 GBq. This source was previously used as an industrial-level gauge and has been collected and securely stored at the CNESTEN storage facility. Table 2 illustrates the principal characteristics associated with this source, to overestimate the radiological exposure, the initial activity has been considered in the calculations.

Table 2. Principal characteristics of ⁶⁰Co source [24].

Principal Characteristics	Source of ⁶⁰ Co
Half-life	5.27 years
Specific activity	4.9 × 10 ¹³ Bq.g ⁻¹
Precursors	^{60m} Co (from ⁶⁰ Fe)
Descendants	⁶⁰ Ni
Principal emission per disintegration (emission probability %)	β ⁻ 318 keV (99.9 %) γ 1 332 keV (100 %) et 1 173 keV (99.9 %)

Methodology

To assess radiation doses throughout the entire dismantling process, we segmented the operation into four distinct exposed tasks, as outlined below, concerning the mentioned time per action or task, which is determined according to previous dismantling operations conducted at CNESTEN's radioactive waste

management facilities. The different tasks are summarized in Fig. 3.

Transport DSRs from temporarily storing radioactive waste to the treatment facility. The duration of this task can vary from 5 to 30 minutes. Sources are transported using a hands pallet truck, and the source is positioned 40 cm from the soil.

Dismantling operation: This task involves removing the active material from its initial shielding device. The duration of this operation can range from 2 to 12 minutes. In this action, the radioactive source is still in its initial shielding, and it is positioned on the table at a height of 77 cm.

Transfer the active material from its shielding device to behind lead glass shielding. This action typically takes from 2 to 12 seconds. The radioactive source in this step is not shielded but we handle it using pliers, to optimize the external exposure by distance.

Verify through the lead glass the integrity of the radioactive source and its characteristics such as reference date, radioelement, and manufacturer. The verification process usually takes from 5 to 30 seconds. In this final action, the radioactive source is bare but behind the lead and lead glass (see Fig. 2).

As the operator moved down the x-axis, the Pythagorean Theorem was used to determine the distances a, b, c, and d between the source and each of the four detectors positioned in the body (see Fig. 4).

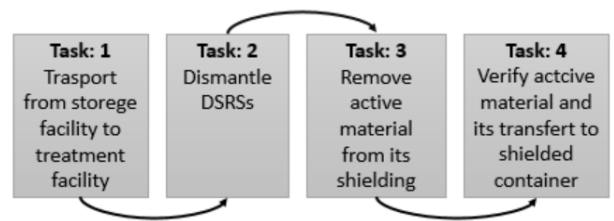


Fig. 3. Flowchart recapitulating the dismantling process operation.

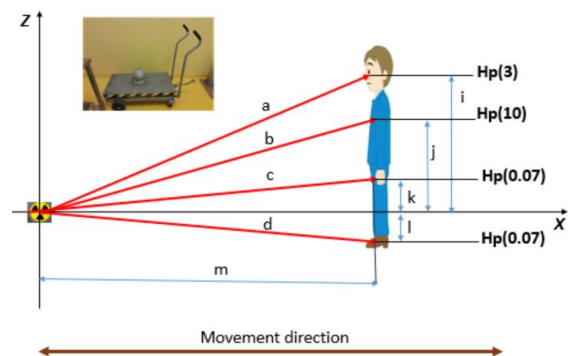


Fig. 4. Detectors positions (whole body and extremities) as a function of distance.

The proposed approach is not unique, some processes may involve more than four tasks. Also in certain instances, we may encounter sources that require additional time. However, it remains a beneficial approach for assessing radiological exposure. A benchmark with regulatory limits was conducted to investigate and analyze professional exposure integrated by workers. As stated in the radiation protection decree, occupational exposure should not exceed the following limits: an effective dose of 20 mSv per year on average over five consecutive years, an effective dose of 50 mSv in only one year, an equivalent dose to the lens of the eye of 150 mSv in only one year, and an equivalent dose to the extremities (hands, feet) or the skin of 500 mSv in one year [25]. Concerning the body segment lengths, parameters from Drillis and Contini are employed in this study [26]. the adopted computational phantoms outlined in the ICRP publication 110 [27-29].

Theoretical aspect

The particle fluence rate $\dot{\Phi}$ ($\text{p.m}^{-2}.\text{s}^{-1}$) is the quotient of $d\Phi$ by dt where $d\Phi$ is the increment of the fluence in the time interval dt [30] in Eq. 1:

$$\dot{\Phi} = \frac{d\Phi}{dt} = \frac{d^2 N}{da dt} \tag{1}$$

For a point source of activity A (Bq) emitting photons of energy E_γ with an intensity $I_\gamma(\%)$, the fluence rate at distance d (m) in Eq. 2:

$$\dot{\Phi} = \frac{A \cdot I_\gamma}{4 \cdot \pi \cdot d^2} \tag{2}$$

To calculate the operational quantities, Eq. 3 can be used [31].

$$\dot{H} = h_\phi * \dot{\Phi} \tag{3}$$

where \dot{H} is the equivalent dose rate (Sv/h), h_ϕ is the conversion coefficient from fluence to equivalent dose rate ($\mu\text{Sv.cm}^2$), and then $\dot{\Phi}$ is the fluence rate.

RESULT AND DISCUSSION

The initial step in the dismantling process involves transferring DSRs from temporary storage to the treatment facility building. The potential operator positions start from the contact of the source (7 cm) to 247 cm, with a step of 40 cm. Equivalent dose rates are calculated for the lens of the eye, the whole body at the chest, and the extremities at hands and feet levels. The simulated Number of Particle Histories (NPS) was 5×10^7 using the NPS card, and the obtained standard deviations ranged between 0.08 % and 0.2 %.

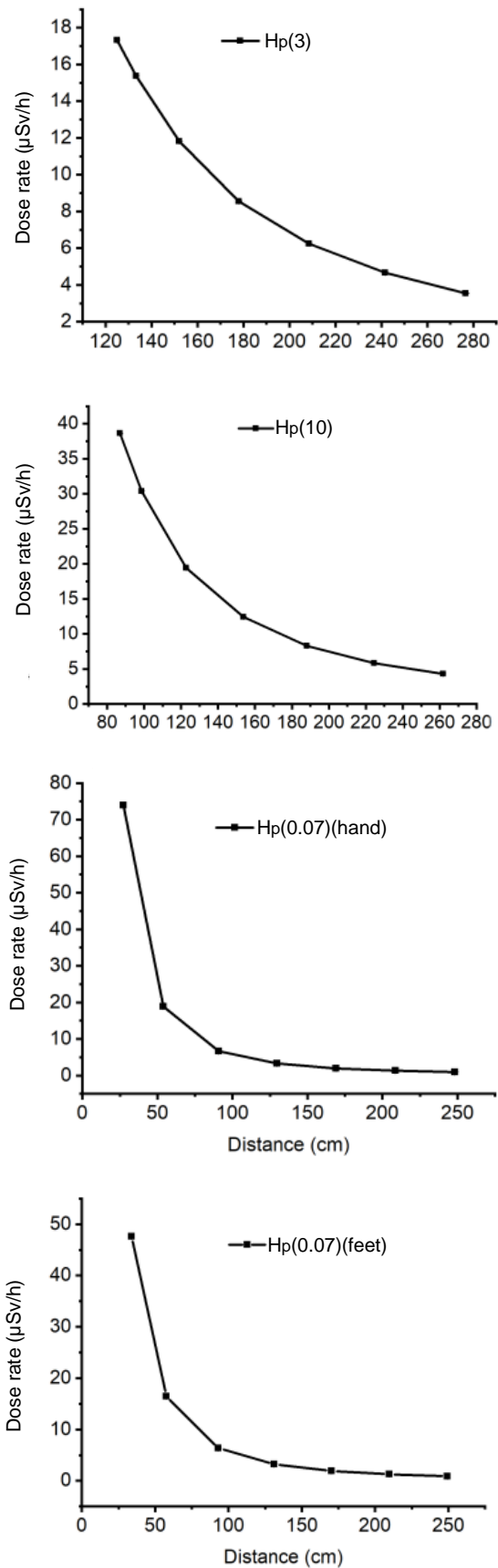


Fig. 5. Operational quantities evaluation at different distances from the source (task one).

In Fig. 5, upon initial examination of the graph, it becomes evident that the dose rate decreases with

distance. When the operator is positioned adjacent to the radioactive source, which is shielded by 7 cm of lead, the detector positions of the lens of the eye, chest, hands, and feet are 27.27 cm, 33.87 cm, 87.00 cm, and 124.93 cm, respectively. The registered dose rates are 74.01 $\mu\text{Sv/h}$, 47.62 $\mu\text{Sv/h}$, 38.64 $\mu\text{Sv/h}$, and 17.33 $\mu\text{Sv/h}$ at hands level, feet, chest, and at the lens of the eye level respectively. Regarding the dose rate curve at the level of the lens of the eye and the chest, their decreasing slopes as a function of distance is nearly similar. However, at the extremities such as the hands and feet, we observe a remarkable drop in the dose rate exactly for the two first steps from the source. This can be explained by the solid angle effect, as the two detectors of the extremities (hands and feet) are closer to the source than the other detectors. Another reason, in the MCNP calculation the source is considered as isotropic, but it is surrounded by 7 cm of lead, which can affect the distribution of the dose rate around the source.

Three essential means of protection against external radiological exposure namely exposure time, distance, and shielding. In scenarios involving ionizing radiation, such as our current situation, where the dismantling process entails a non-negligible level of exposure, optimizing radiation safety relies on managing these parameters effectively. Depending on the exposure circumstances, we may prioritize either time, distance, or shielding. Sometimes, a combination of two factors can be managed simultaneously. For instance, optimizing radiation dose can involve adding shielding and minimizing the duration of exposure. Analysis of four graphs depicting dose rate as a function of both exposure time and distance, Figs. 6 to 9 demonstrates that reducing exposure time and increasing distance between the worker and radioactive source significantly diminishes occupational exposure levels, it is clear that the dose follow an exponential decrease as a function of distance and exposure time. To emphasize the distance effect, 240 cm contributed to reducing the dose rate with 20.40 % at the lens of the eye, 11.11 % at the chest (whole body), 1.21 % at the hands, and 1.87 % at the feet. From a radiation protection point of view, it is better to slightly overestimate the dose than to underestimate. This is why, if we consider that the worker spent 30 minutes on this task and an average distance of 40 cm, the worker will receive an effective dose of 15.19 μSv , 7.68 μSv at the lens of the eye, and extremities 9.43 μSv and 8.23 μSv simultaneously at hands and feet. In this task, it is possible to optimize the dose rate, but it depends on the campaign, if sources are with an important activity, and the number of sources is important we can opt to add a layer of lead surrounding the source.

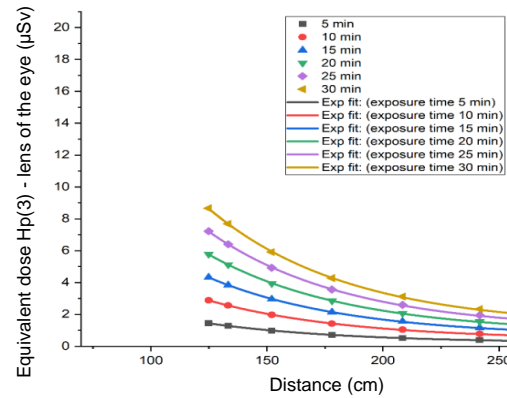


Fig. 6. Equivalent dose Hp(3) – lens of the eye, as a function of the distance and exposure time.

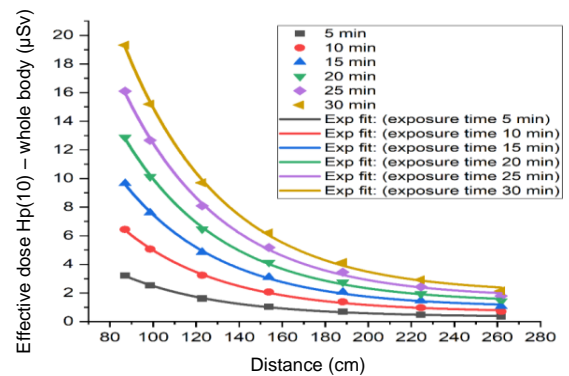


Fig. 7. Equivalent dose Hp(10) - whole body, as a function of the distance and exposure time.

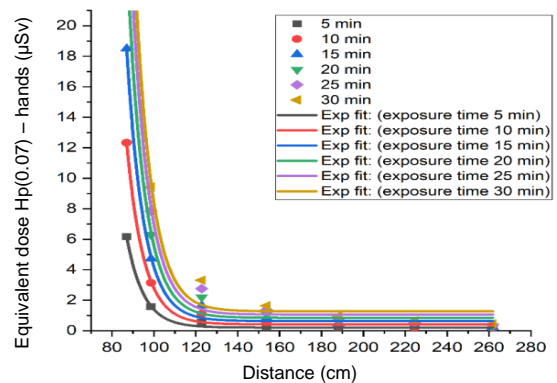


Fig. 8. Equivalent dose Hp(0.07) - hands, as a function of the distance and exposure time.

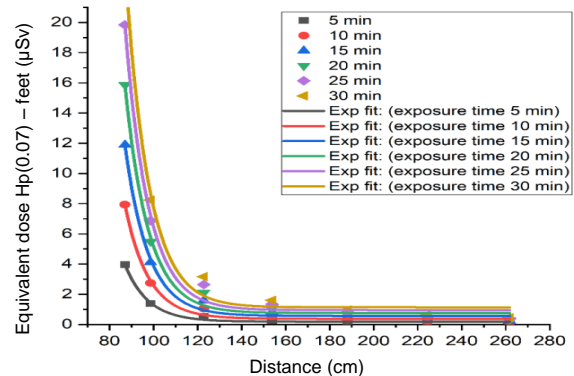


Fig. 9. Equivalent dose Hp(0.07) – feet, as a function of the distance and exposure time.

In Task 2, workers handle the DSRS directly, even though the source remains shielded with 7 cm of lead at this stage. As illustrated in Fig. 10, hands receive the highest exposure as they come into direct contact with the source. In certain cases, the worker may use lead gloves to mitigate external exposure to their hands. Spending 24 minutes on this task results in a dose of 375.02 μSv , which accounts for 0.075 % of the annual regulatory limit. The effective whole-body dose stands at 38.89 μSv , representing 1.94 % of the limit, while the dose to the lens of the eye is 16.42 μSv , just 0.01 % of the limit. Feet exposure, comparatively, is negligible, at 1.54 μSv , accounting for 3.08×10^{-4} % of the limit.

In Task 3, workers handle a bare DSRS without any shielding, leading to significantly higher dose rates. At the point of manipulation, the dose rates for the lens of the eye, whole body, hands, and feet are 1117.45 $\mu\text{Sv/h}$, 3121.59 $\mu\text{Sv/h}$, 6186.38 $\mu\text{Sv/h}$, and 1123.08 $\mu\text{Sv/h}$ respectively. A key advantage of this step is the short exposure time, typically between 2 to 12 seconds, making it more manageable. Considering a 12 second, the integrated doses for the lens of the eye, whole body, hands, and feet are 3.72 μSv , 10.40 μSv , 20.62 μSv , and 0.37 μSv , respectively, as presented in Fig. 11. In 6.4 hours of exposure, the worker reaches the annual whole-body limit.

Moving to Task 4, the source is exposed but shielded behind lead and leaded glass. While this shielding offers significant protection to the whole body, the lens of the eye, and feet, hands remain vulnerable due to direct exposure. Dose rates for the lens of the eye and the whole body remain under 10 $\mu\text{Sv/h}$ as demonstrated in Fig. 12, whereas for the hands, the dose rate climbs to 5369.24 $\mu\text{Sv/h}$, and for feet, about 94.48 $\mu\text{Sv/h}$. Given the brief duration of this task, typically 5 to 30 seconds, integrated doses in 30 seconds, for the lens of the eye, whole body, hands, and feet are 0.05 μSv , 0.07 μSv , 44.74 μSv , 0.79 μSv , respectively.

The contribution of each task to the overall exposure of the simulated operational quantities is depicted in Fig. 13. The considered durations in the calculation of the generated doses are the maximum such as 30 minutes, 30 minutes, 12 seconds, and 30 seconds for tasks 1, 2, 3, and 4, respectively. To optimize external exposure, several preparatory actions are advised to be taken before commencing operations, including assessing doses using simulation tools, preparing individual and collective protective equipment, ensuring the availability of individual and collective radiological monitoring equipment, and gathering all necessary

materials for DSRS dismantling. During the dismantling operation, it is essential to adhere to good practices, such as utilizing appropriate dose rate meters, conducting continuous dose rate measurements at workers' positions, performing dose rate mapping around the workplace, and meticulously controlling and recording the doses received by workers.

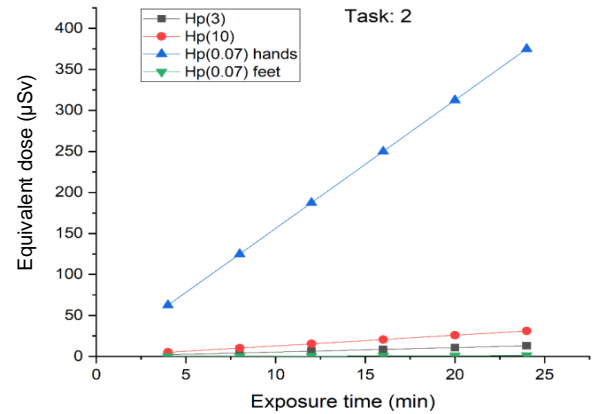


Fig. 10. Equivalent dose (Hp(3), Hp(10), Hp(0.07) for hands and feet, as a function of exposure time (Task 2).

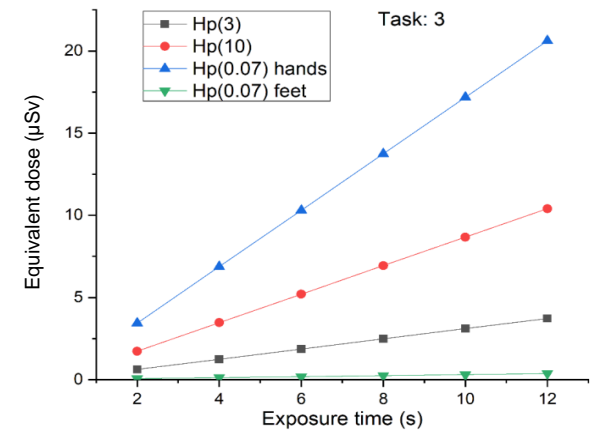


Fig. 11. Equivalent dose (Hp(3), Hp(10), Hp(0.07) for hands and feet, as a function of exposure time (Task 3).

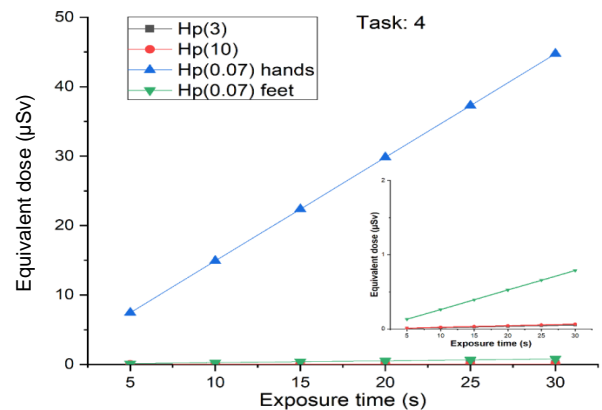


Fig. 12. Equivalent dose (Hp(3), Hp(10), Hp(0.07) for hands and feet, as a function of exposure time (Task 4).

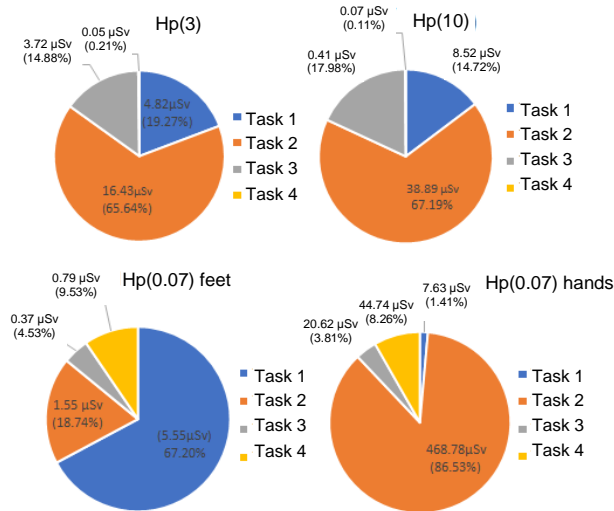


Fig. 13. The contribution of each task to the overall exposure for each operational quantity.

CONCLUSION

This study underscores the importance of a rigorous radiological exposure assessment in effectively managing DRSs. The inherent hazards of DRS demand meticulous planning and the implementation of robust management plans to safeguard both workers and the environment. The comprehensive evaluation of operational tasks and radiological exposure levels has identified critical areas for enhancing occupational radiation protection measures and enabled us to discover the more critical step in the dismantling process and to know the more exposed organs in the body in each task. By dismantling the investigated source in this study, workers can maintain compliance with regulatory requirements, achieving exposure levels of 4.17 %, 72.35 %, 27.09 %, and 0.41 % from the daily limit dose for the lens of the eye, chest, and extremities at hands and feet respectively. Moreover, by optimizing doses through minimizing exposure time and potentially enabling the dismantling of multiple DRSs per day, our approach can significantly enhance operational efficiency and worker safety. Future works will involve the assessment of other gamma emitters like ¹³⁷Cs in one hand, and on other hand a possible evaluation of neutron emitters such as Troxler with ¹³⁷Cs / ²⁴¹Am-⁹⁰Be, which still pose a challenge.

ACKNOWLEDGMENT

We extend our thanks to the radioactive waste management team at CNESTEN, particularly Ms. ELGHAILASI and M. FADIL, for their availability during this study.

REFERENCES

- IAEA, Management of disused sealed radioactive sources, International Atomic Energy Agency, Vienna (2014).
- J. C. Benitez-Navarro, J. Canizares, E. Demireva et al., Current Approaches on the Management of Disused Sealed Sources in Bulgaria, in: BULATOM International Nuclear Forum: The Future of Nuclear Energy on the Balkans: Security of Energy Supply and Nuclear New Builds, Bulgaria (2005) 1.
- IAEA, Governmental, Legal and Regulatory Framework for Safety, International Atomic Energy Agency, Vienna (2016).
- IAEA, Categorization of Radioactive Sources IAEA Safety Standards Series No. RS-G-1.9, International Atomic Energy Agency, Vienna (2005) 70.
- K. Raj, K. K. Prasad and N. K. Bansal, Nucl. Eng. Des. **236** (2006) 914.
- IAEA, Policies and Strategies for Radioactive Waste Management, International Atomic Energy Agency, Vienna (2009) 68.
- D. Telleria and G. Proehl, Atom Indones. **39** (2014) 101.
- IAEA, Predisposal Management of Radioactive Waste, General Safety Requirements Part 5, International Atomic Energy Agency, Vienna (2009).
- IAEA, Guidance on the Management of Disused Radioactive Sources, Guid. Manag. Disused Radioactive Sources, International Atomic Energy Agency, Vienna (2018) 1.
- O. Kabach, A. Chetaine and A. Benchrif, Int. J. Nucl. Secur. **6** (2020) 1.
- S. Uras, C. Zovini, A. Paratore et al., State of the Art in Packaging, Storage, and Monitoring of Cemented Wastes, Roma (2021) 1.
- A. N. Yusupov, P. A. Mikhailov, V. D. Kizin et al., Yad. Energ. (2023) 95.
- IAEA, The Safety Case and Safety Assessment for the Predisposal Management of Radioactive Waste, No. GSG-3, International Atomic Energy Agency, Vienna (2013).
- B. El Azzaoui, H. Hamdane, R. Outayad et al., J. Mater. Environ. Sci. **14** (2022) 1425.
- IAEA, Radiation Protection and Safety of Radiation Sources: International Basic Safety Standards, International Atomic Energy Agency, Vienna (2014).

16. A. Putri, R. Zurma, R. Munir *et al.*, Atom Indones. **49** (2023) 185.
17. A. Taopik, L. E. Lubis, D. S. K. Sihono Atom Indones. **49** (2023) 169.
18. Muslim, F. I. Maulana, H. Suseno *et al.*, Atom Indones. **48** (2022) 231.
19. Y. O. Salem, Etude expérimentale et modélisation Monte Carlo des grandeurs opérationnelles en métrologie des rayonnements ionisants : application à la dosimétrie neutrons par radiophotoluminescence, Université de Strasbourg, (2014).
20. ICRU, Appendix A. Values of Conversion Coefficients, Journal of the ICRU. **20** (2020) 46.
21. B. El Azzaoui, M. Y. Messous, A. Didi *et al.*, Int. J. Power Energy Convers. **14** (2023) 376.
22. C. J. Werner, MCNP User's Manual, Code Version 6.2, Report la-UR-17-29981, Los Alamos National Laboratory (2017).
23. R. J. McConn Jr, C. J. Gesh, R. T. Pagh *et al.*, Compendium of Material Composition Data for Radiation Transport Modeling. PNNL-15870 Rev. 1 (2011).
24. M. J. Berger *et al.*, XCOM: Photon Cross Sections Database, NIST, PML, Radiation Physics Division (2010).
25. AMSSNuR, La protection de la population, des travailleurs et de l'environnement contre les dangers résultant de l'exposition aux rayonnements ionisants, décret n°2.23.151, Morocco (2023).
26. P. Bannier, H. Jin and P. M. Goodrum, J. Inf. Technol. Constr. **21** (2016) 292.
27. M. N. AL-Suhbani, N. E. H. Baghous, S. Serag, *et al.*, Atom Indones. **1** (2024) 1.
28. M. T. Saidin, A. A. Rahman, H. H. Harun *et al.*, Atom Indones. **47** (2021) 213.
29. ICRP, ICRP Publication 110, Adult Reference Computational Phantoms, International Commission on Radiological Protection (2009).
30. J. P. Seuntjens, W. Strydom and K. R. Shortt, Chapter 2, Dosimetric Principles, Quantities and Units, International Atomic Energy Agency (2005).
31. R. Behrens, J. Radiol. Prot. **32** (2012) 455.